RESEARCH ARTICLE

Design and Analysis of Z-Trench-Assisted 9-LP-Mode Fiber With Low Differential Modal Group Delay and High Spatial Density

YUHENG XIE [ID], JIANJUN TANG, QI ZHAO, LIPENG FENG, AND TIANQI DOU
Institute of Basic Operations Technology, China Telecom Research Institute, Beijing 102200, China

Corresponding author: Yuheng Xie (xieyh@chinatelecom.cn)

ABSTRACT We present a novel Z-trench-assisted (Z-TA) graded index 9-LP-mode fiber that significantly suppresses the maximum absolute differential modal group delay (Max |DMGD|) while obtaining a high normalized spatial density (NSD). The finite element method (FEM) is applied for numerical simulations, and the results show that the Max |DMGD| is 18.9-ps/km at 1550-nm. To the best of our knowledge, it is improved by more than 30% compared to that of the theoretical optimal value in TA structure so far. Furthermore, the NSD of the proposed fiber can reach 44.64 at 1550-nm. Over the C band, the Z-TA 9-LP-mode fiber exhibits Max |DMGD| < 32.6-ps/km, mode field area (A_{eff}) > 100 μm^2 and low bending loss. In addition, the Z-TA structure is able to maintain relatively low degradation of DMGD characteristics when strict manufacturing variabilities are considered.

INDEX TERMS Few-mode fiber, differential mode group delay, Z-trench-assisted, normalized spatial density, mode division multiplexing.

I. INTRODUCTION

Mode division multiplexing (MDM) using few-mode fiber (FMF) is one of the main implementations of space division multiplexing (SDM) technology, which can effectively cope with the capacity crisis of single-mode fiber systems [1], [2], [3]. With the advantage of parallel channels brought by multiple spatial modes, FMF has also become an important choice for co-fiber transmission between classical and quantum signals in continuous-variable quantum key distribution [4]. Note that the differential modal group delay (DMGD), caused by the different propagation constants of each LP mode, is a crucial indicator of FMF. Depending on the magnitude of DMGD, FMFs can be distinguished into two types, one with large DMGDs between LP modes and the other with DMGDs as close to zero as possible. The former reduces the intermodal crosstalk through large effective index difference (Δn_{eff}) between LP modes, thus decreasing the mode coupling [5], [6]. However, due to the accumulation of large modal delays, such FMFs are more suitable for

The associate editor coordinating the review of this manuscript and approving it for publication was Sukhdev Roy.

scenarios including data centers and computer rooms rather than long-distance transmission.

Conversely, low DMGD may increase the risk of distributed mode coupling along the line, where the modes need to be separated by multiple-input multiple-output (MIMO) at the receiver. The storage pressure and tap numbers of MIMO equalizers can be alleviated by suppressing the DMGD, thus reducing the complexity of long-haul strongly coupled MDM systems [7]. To reduce DMGD, trench-assisted graded index (TA-GI) profile has been widely used. In [8], a TA-GI 6-LP-mode fiber is successfully fabricated with DMGD of about 69 ps/km in C band and 124 ps/km in $C+L$ band. An optimal value of Max |DMGD| < 10 ps/km at 1550 nm is numerically achieved for a TA-GI 6-LP-mode fiber with core radius of 14 μm and normalized frequency $V = 9.65$ [9]. In [10], a TA-GI FMF is able to support 9-LP modes with theoretical DMGDs of 24.4 ps/km. However, these low-DMGD designs are known to be very sensitive to profile variations that occur during the actual fabrication [9], [10]. For example, the manufacturing tolerance results in a Max |DMGD| of greater than 100 ps/km for the optimized 6-LP-mode fiber with Max |DMGD| < 10 ps/km. The Max |DMGD| < 155 ps/km is
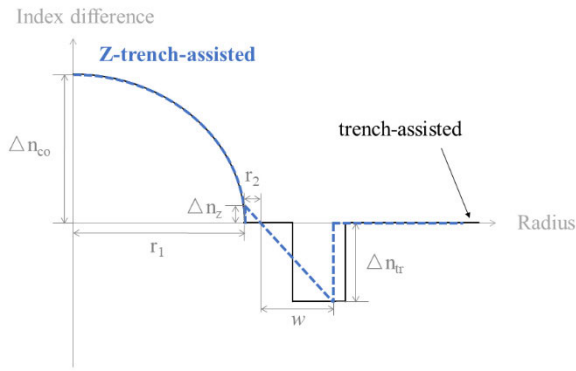
FIGURE 1. Schematic index profile of the Z-TA and TA structure graded index 9-LP-mode fiber.

experimentally obtained for the optimized 9-LP-mode fiber with Max |DMGD| < 25 ps/km. One can see that the actual DMGD is almost 6 to 10 times larger than the theoretical minimum, which would greatly increase the instability and difficulty of mass production.

In this paper, we propose a novel Z-trench-assisted (Z-TA) graded index 9-LP-mode fiber to enhance the constraint of the auxiliary structure on specific higher-order modes fields, thereby reducing the Max |DMGD| evidently. In particular, low DMGD, high spatial density and tight fabrication tolerances are considered simultaneously. The modeling and numerical simulation of the designed FMF is analyzed by COMSOL Multiphysics software based on full vector finite element method (FEM). The mode effective refractive index is calculated with an accuracy of 10^{-4} and the free triangular mesh with extremely fine unit size is used. In section II, the dependence of Max |DMGD| on the Z-TA structural parameters is demonstrated. The Max |DMGD| is 18.9 ps/km at 1550 nm, to the best of our knowledge, it achieves an optimization of more than 30% compared to that of the theoretical optimal value in TA structure so far. Section III investigates the broadband performance of the proposed fiber, with the NSD of 44.64 at 1550 nm and relatively low bending loss. Over the C band, the Max |DMGD| is less than 32.6 ps/km. When the discussed fabrication variabilities are 3 times the standard deviation, numerical calculations show that the Z-TA structure is able to keep the degradation of DMGD characteristics less than 5 times of the designed value. The main conclusions are summarized in section IV.

II. Z-TA STRUCTURE AND DMGD

Figure 1 shows the schematic diagram of the refractive index distribution of the proposed Z-TA structure 9-LP mode fiber (blue dashed line), and as a comparison, the black solid line represents that of the TA structure. Where Δn_{co}, r_1, r_2, Δn_z, w and Δn_{tr} denote core-cladding index difference, core radius, core-trench distance, the index difference between Z-structure and cladding, Z-trench width and trench-cladding index difference, respectively. It can be seen that the Z-trench is a structure whose refractive index distribution changes gen-

tly from positive to negative, with the intention of changing the power distribution of specific higher-order modes and thus further reducing the DMGD. The index profile $n(r)$ is given by:

$$n(r) = \begin{cases} n_{co}[1 - \Delta n_{co}(r/r_1)^{\alpha}], & 0 \leq r \leq r_1 \\ \dfrac{r_1 + r_2 - r}{r_2}n_z, & r_1 \leq r \leq r_1 + r_2 \\ \dfrac{r - r_1 + r_2}{w}n_{tr}, & r_1 + r_2 \leq r \leq r_1 + r_2 + w \\ n_{cl}, & r \geq r_1 + r_2 + w \end{cases}$$

(1)

where n_{co}, α, n_z, n_{tr} and n_{cl} represent core index, profile exponent, Z-trench index, trench index and cladding index, respectively. For 9-LP-mode fibers, the normalized frequency V is set to 11.8, which is generally the maximum value that makes 9-LP modes operate robustly [10], [11]. The core-cladding index difference and core radius can be adjusted according to V when $\alpha = 1.94$, that is, $\Delta n_{co} = 14.9 \times 10^{-3}$ at 1550 nm and $r_1 = 14$ μm [10], [11], [12], [13].

As the core parameters are determined, the dependence of Max |DMGD| on Z-TA structural parameters are investigated. The DMGD is obtained by subtracting the group delay τ of LP_{mn} from that of LP_{01}. Since τ refers to the time required for an optical pulse to travel a unit axial distance, DMGD can be calculated by the following equation [14], [15]:

$$DMGD = \frac{n_{effLP_{mn}} - n_{effLP_{01}}}{c} - \frac{\lambda}{c}\left(\frac{\partial n_{effLP_{mn}}}{\partial \lambda} - \frac{\partial n_{effLP_{01}}}{\partial \lambda}\right)$$

(2)

where n_{eff} is the effective index of the modal group, c is the light velocity in a vacuum and λ means the wavelength. Therefore, the Max |DMGD| is the absolute value of the difference between the maximum positive and negative values of DMGD in all transmission modal groups. Figure 2 shows, for these core parameters, the relationship between the Max |DMGD| and r_2 at 1550 nm when the initial $\Delta n_z = 0.2\%$, $w = 4$ μm and $\Delta n_{tr} = -6 \times 10^{-3}$, respectively. For TA structure, the Max |DMGD| first drops visibly and then grows slightly as r_2 increases from 0.6 μm to 1.2 μm, reaching an optimized value of ~25 ps/km at $r_2 = 0.9$ μm. In contrast, the Max |DMGD| of lower than 25 ps/km can be obtained in the proposed Z-TA structure when r_2 ranges from 0.85 μm to 1.05 μm. It should be noted that the Z-TA structure is able to get a lower Max |DMGD| while retaining a larger r_2 tolerance range. Here, r_2 is set to 0.95 μm for subsequent analysis.

Figure 3 shows the color map of Max |DMGD| dependence on w and Δn_{tr} at 1550 nm, where the dark blue region indicates Max |DMGD| < 25 ps/km. When $r_2 = 0.95$ μm, w of greater than 1.7 μm and Δn_{tr} of less than -0.58% can meet the requirement of Max |DMGD| below 25 ps/km. In addition, a lower Δn_{tr} helps to reduce Max |DMGD| significantly and allows a larger range of w. The concept of trench volume
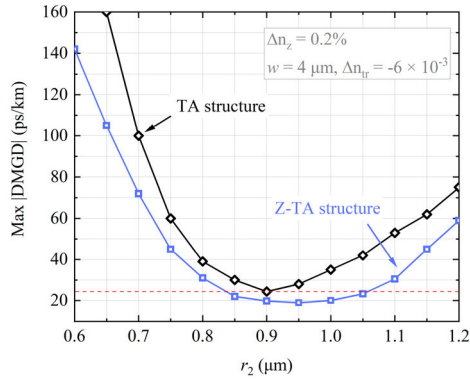
FIGURE 2. The relationship between Max |DMGD| and r2 at 1550 nm when the initial Δn_z = 0.2%, w = 4 μm and Δn_{tr} = -6 × 10-3, respectively.
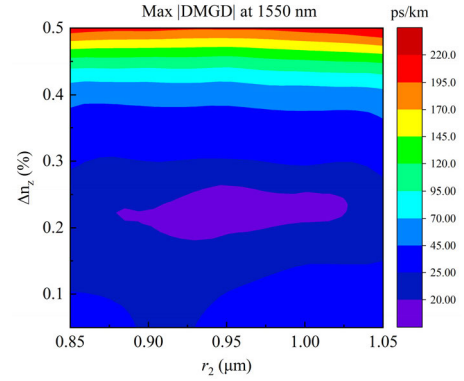

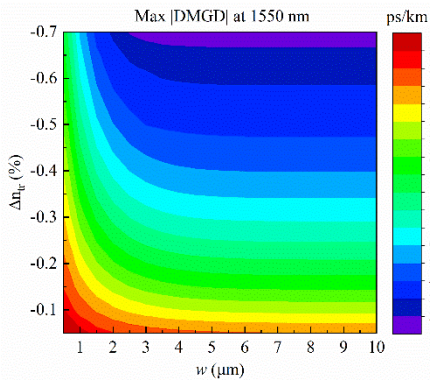**FIGURE 3.** The color map of Max |DMGD| dependence on w and Δn_{tr} at 1550 nm. (The dark blue region means the Max |DMGD| < 25 ps/km).
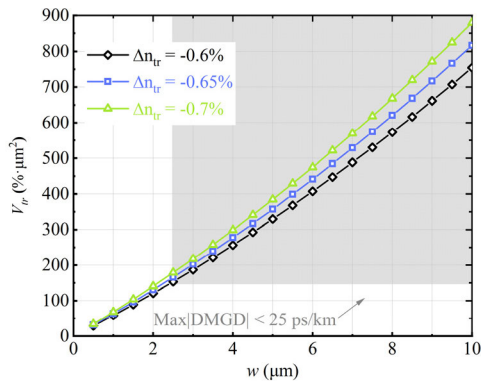

FIGURE 4. The variation of V_{tr} with w and Δn_{tr} at 1550 nm.

is introduced to further evaluate the relationship between Max |DMGD| and trench parameters. The trench volume is the integral of Δn_{tr} over the trench cross section, and it is defined as [16] and [17]:

$$V_{tr} = \left| 2\pi \times \int_{r_1+r_2}^{r_1+r_2+w} \Delta_{tr}\%(r) \times r \times dr \right| \quad (3)$$

in which r is the distance to the axis.

Figure 4 depicts the variation of trench volume with trench parameters at 1550 nm, the black line, blue line and green line represent Δn_{tr} = -0.6%, Δn_{tr} = -0.65% and
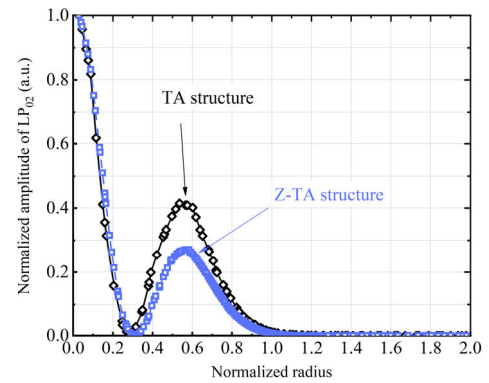

FIGURE 5. The dependence of Max |DMGD| on r2 and Δn_z at 1550 nm.

FIGURE 6. The normalized amplitude versus the normalized radius of LP02 mode. (The black line and blue line indicate the case of the theoretical TA structure and our design).

Δn_{tr} = -0.7%, respectively. The trench volume of greater than 150 %· μm^2 is sufficient to keep Max |DMGD| below 25 ps/km. Note that the trench volume not only contributes to the reduction of Max |DMGD|, but it also affects the bend losses of higher-order modes and cut-off of the unwanted modes. A detailed discussion of this part will be explained in section III. Here, we set V_{tr} = 300 %· μm^2 to bound Max |DMGD| without adjusting the bending performance of guided modes significantly.

The dependence of Max |DMGD| on r_2 and Δn_{ht} at 1550 nm is calculated in Fig. 5. The Δn_z of higher than 0.3% leads to a sharp increase in Max |DMGD| as more energy from the higher order modes is transferred to the Z-TA structure. The combinations of r_2 from 0.85 μm to 1.05 μm and Δn_z from 0.13% to 0.27% can reduce Max |DMGD| below 25 ps/km. Furthermore, the purple region indicates that the Max |DMGD| is less than 20 ps/km, with a typical value of 18.9 ps/km. In order to have flexible parameter tolerances, r_2 = 0.95 μm and Δn_z = 0.22% are chosen. As a result, the Max |DMGD| of the Z-TA 9-LP-mode fiber is reduced by more than 30% (25/18.9) compared to that of the theoretical optimal value in TA structure.

Figure 6 simulates the relationship between normalized amplitude of LP$_{02}$ mode and the normalized radius (ratio
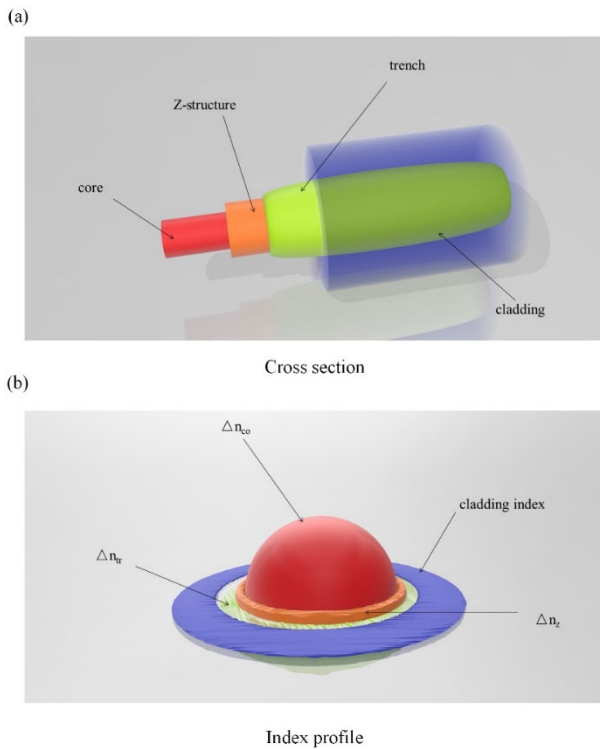
(a)

(b)

FIGURE 7. The three-dimensional diagram of (a) the cross section and (b) the index profile of the Z-TA 9-LP-mode fiber.
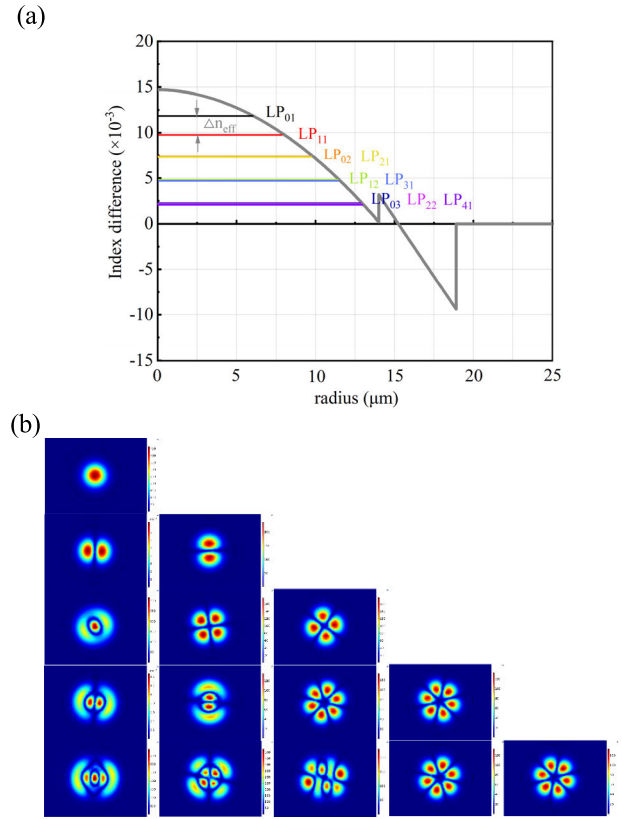
(a)

(b)

FIGURE 8. (a) The index profile of the optimized Z-TA 9-LP-mode fiber and the n_{eff} of LP modes at 1550 nm; (b) the electric field intensity of LP modes at 1550 nm.

to r_1) from the perspective of mode power distribution, where the black line represents the theoretical TA structure and the blue line is our design. In principle, the expansion of the electric field of higher-order modes into the cladding is the main reason for the increase of DMGDs in FMFs [18], [19]. The results show that the mode field distribution of our design is more concentrated, and the energy can be better confined in the Z-TA structure. Therefore, the DMGDs of the specific LP modes will be further reduced by increasing the n_{eff} of that modes.

III. BROADBAND CHARACTERISTICS OF Z-TA 9-LP-MODE FIBER

Figure 7 shows the cross section and index profile of the Z-TA 9-LP mode fiber in a more visual three-dimensional form. Due to the precise multilayer core structure, the Plasma Chemical Vapor Deposition (PCVD) is more suitable as one of the methods to fabricate the proposed fiber [20], [21].

The optimized index profile and electric field intensity of Z-TA 9-LP-mode fiber at 1550 nm are shown in Fig. 8(a) and 8(b), respectively. The minimum Δn_{eff} of adjacent modal groups is 2.38×10^{-3} (LP$_{01}$ vs. LP$_{11}$), and the highest modal groups (LP$_{03}$, LP$_{22}$ and LP$_{41}$) can operate robustly since the index difference between their n_{eff} and n_{cl} is $\sim 2.3 \times 10^{-3}$. Figure 9 depicts the broadband characteristics of DMGDs and the Max |DMGD| versus wavelength on the *C* band. The refractive index of SiO_2, GeO_2-SiO_2 and F-doped SiO_2 at different wavelengths can be calculated from the hybrid Sell-
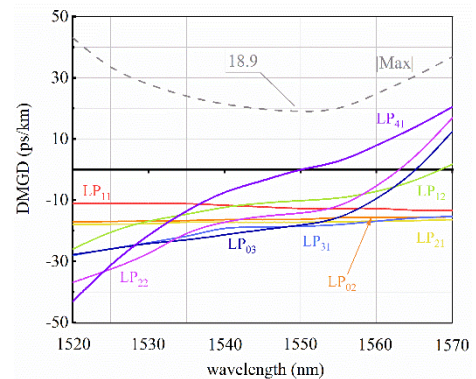

FIGURE 9. The DMGDs vs. wavelength of the optimized Z-TA 9-LP-mode fiber over the C band. (The solid lines mean the DMGDs of LP modes and the dashed line is the Max |DMGD|).

meier equation describing the dependence of the refractive index on wavelength and doping concentration (mol%) [22], which can also be found in [23]. It can be seen that DMGDs of lower-order modes grow more slowly than those of LP$_{03}$, LP$_{22}$ and LP$_{41}$ at long wavelengths. The Max |DMGD| at 1550nm and the entire *C* band is 18.9 ps/km and 32.6 ps/km, respectively. Furthermore, the DMGD slope is less than |1.22| ps/km/nm (LP$_{41}$) in the range of 1520 nm to 1570 nm.
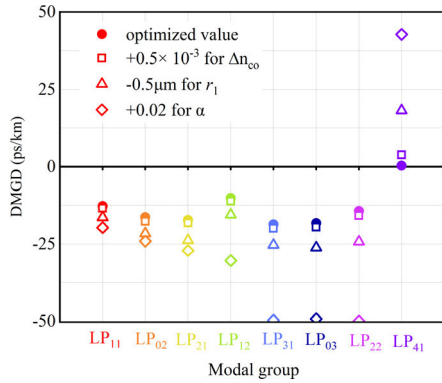
FIGURE 10. The optimized DMGDs and DMGDs with fabrication tolerances of Z-TA 9-LP mode fiber at 1550 nm. (Red dots: the optimized values, open squares: +0.5 × 10-3 for core-cladding index difference, open triangles: -0.5 μm for core radius and open diamonds: +0.02 for alpha).

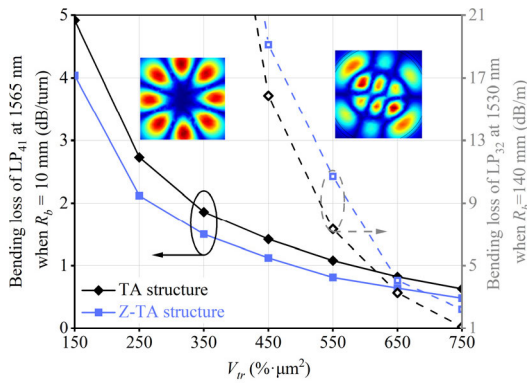**FIGURE 11.** The bending loss of the highest-order guided mode LP41 at 1565 nm when Rb = 10 mm and the bending loss of the leaky mode LP32 versus **V$_{tr}$** at 1530 nm when Rb = 140 mm. (The black lines represent the bending loss of the modes in TA structure 9-LP-mode fiber, the blue lines mean that the bending loss of our proposed fiber).

The sensitivity of DMGD to profile variation may prevent it from reaching the optimized low values. To evaluate the production variations on the Z-TA 9-LP-mode fiber, three times the standard deviations (σ) are considered, including +0.5 × 10^{-3} for index differences, -0.5 μm for radius and +0.02 for α [9], [12]. Figure 10 shows the optimized DMGDs and DMGDs with fabrication tolerances of the proposed fiber at 1550nm. The fluctuation of α cause the largest increase in DMGDs relative to the changes of other parameters, and the worst Max |DMGD| is 93.4 ps/km. It is noticeable that the worst Max |DMGD| of the proposed fiber is less than 5 times the designed value under the conditions of such strict deviations, compared to the general case where the DMGD with fabrication tolerances is higher than 6 to 10 times the theoretical optimal value. In addition, the worst Max |DMGD| that occurs in actual production will be much lower than the results obtained from our numerical simulations, since the tolerances of mature fiber manufacturing process are only half of 3σ [9].

TABLE 1. The optimIZED fiber parameters with fabrication tolerances.

Symbol	Fiber parameters
r_1	14.0 μm
Δn_{co}	14.9 × 10^{-3}
α	1.94
r_2	0.85 μm to 1.05 μm
Δn_z	0.18% to 0.26%
V_{tr}	250 %·μm^2 to 550 %·μm

The auxiliary structures are not only used to fulfill specific functionality, but also to ensure low macro-bend losses for all guided modes and high losses for the unwanted modes to guarantee their effective cut-off. Here, the bending loss should be <10 dB/turn at 10 mm bend radius (R_b) for LP$_{41}$ at 1565 nm while it should be > 19.34 dB on a 22 m sample with 1 loop of $R_b \geq$ 140 mm for the leaky mode LP$_{32}$ at 1530 nm [14]. Fig. 11 shows the bending loss of the highest-order mode LP$_{41}$ and the leaky mode LP$_{32}$ dependence on V$_{tr}$. The black solid and dashed lines correspond to the bending loss of the modes in TA structure as reference, and the blue solid and dashed lines represent the bending loss of our design. The bending loss of LP$_{41}$ is less than 5 dB/turn when V$_{tr} \geq$ 150 %· μm^2. Furthermore, V$_{tr} \leq$ 550 %· μm^2 is sufficient to cut off the leaky mode stably. Note that the reasonable range of V$_{tr}$ in Z-TA 9-LP-mode fiber should be approximately from 250 %· μm^2 to 550 %· μm^2 to get the optimal DMGDs and meet the required bending loss.

The normalized spatial density (NSD) is used to characterize the space efficiency of SDM fibers and that can be expressed as follows [12]:

$$NSD = \left[\sum_{c=1}^{C} \sum_{m=1}^{M} (A_{eff,m}) \bigg/ (\frac{\pi}{4}D^2) \right] \bigg/ SD_{SSMF} \quad (4)$$

where c is the number of cores, m is the number of spatial modes, D is the fiber diameter. Furthermore, SD$_{SSMF}$ is the spatial density of the standard single mode fiber [12]:

$$SD_{SSMF} = A_{eff} \bigg/ (\frac{\pi}{4}D^2)$$
$$= 80 \mu m^2 \bigg/ [\frac{\pi}{4} \times (125 \mu m)^2] \quad (5)$$

Figure 12 shows the NSD of representative low-DMGD FMFs (blue open diamonds) [9], [10], [24], single-mode MCFs (green open diamonds) [25], [26], [27], few-mode MCFs (green solid diamonds) [28], [29], [30] and our design (red solid circle). The numbers in each square bracket stand for the number of SDM channels and NSD, respectively. For low-DMGD FMFs, strong mode overlapping makes the NSD proportional to the number of LP modes. However, The NSD of MCFs varies greatly depending on the design of D and the arrangement of cores. For example, a 13-core 5-LP modes fiber design (104 SDM channels) with D = 195 μm

TABLE 2. The optimal fiber performance of Z-TA 9-LP-MODE FIBER AT 1550 NM.

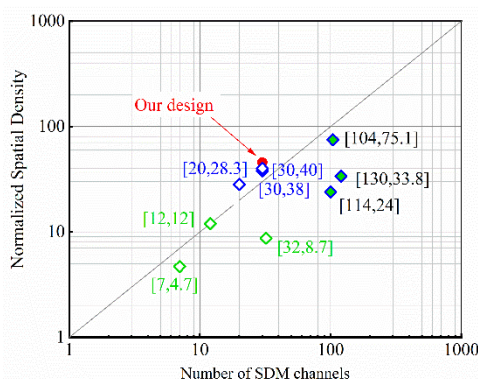|	LP$_{01}$	LP$_{11}$	LP$_{02}$	LP$_{21}$	LP$_{12}$	LP$_{31}$	LP$_{03}$	LP$_{22}$	LP$_{41}$
n_{eff}-cladding index (10^{-3})	12.08	9.7	7.2	7.2	4.7	4.7	2.3	2.3	2.3
Min Δn_{eff} between mode groups (10^{-3})	2.48 (LP$_{21}$ vs. LP$_{12}$)								
DMGD vs.LP$_{01}$ (ps/km)	/	-12.7	-16.3	-17.2	-10.1	-18.6	-18.2	-14.3	0.3
Max |DMGD| (ps/km)	18.9 (LP$_{31}$ vs. LP$_{03}$)								
Bending loss ($R_b = 10$ mm) (dB/turn)	≪1	≪1	≪1	≪1	≪1	≪1	1.04	1.55	1.78
A_{eff} (μm^2)	104	169	214	228	230	232	281	272	239
Dispersion [ps/(nm·km)]	18.1	18.3	18.6	18.7	19.6	19.7	18.9	19.1	19.3

FIGURE 12. Normalized spatial density vs. number of SDM channels for low-DMGD FMFs (blue open diamonds), MCFs (green open diamonds for single-mode types and green solid diamonds for few-mode types) and our design (red solid circle).

achieves a NSD of 75.1 in [30]. In particular, the NSD of our design reaches the highest value of ~44.64 under the same number of SDM channels attributes to the relatively large A_{eff} of the lower-order modes. Finally, we summarize the optimized fiber parameters with fabrication tolerances and the performance of Z-TA 9-LP-mode fiber (at 1550 nm) in Table 1 and Table 2, respectively.

IV. CONCLUSION

We propose a novel Z-TA graded index 9-LP-mode fiber to adjust the power distribution of specific higher-order modes and enhance the mode field confinement ability of the auxiliary structure, thereby significantly reducing the Max |DMGD| while realizing high spatial efficiency. Numerical results show that the Max |DMGD| is 18.9 ps/km at 1550 nm, to the best of our knowledge, it achieves an optimization of more than 30% compared to that of the theoretical optimal value in TA structure so far. Furthermore, the NSD of the proposed fiber can reach 44.64 at 1550 nm. Over the C band, the Z-TA 9-LP-mode fiber exhibits Max |DMGD|

< ~32.6 ps/km, $A_{eff} > 100$ μm^2 and low bending loss. In particular, when considering tight fabrication variabilities of 3 times the standard deviation, the worst Max |DMGD| of the proposed fiber is less than 5 times the designed value in comparison to the general case where the DMGD with fabrication tolerances is higher than 6 to 10 times the theoretical optimal value. Therefore, the possible fluctuations in actual production are acceptable and predictable. With the perspective of these performances, we believe that the Z-TA graded index 9-LP-mode fiber can be used in long-haul strongly coupled MDM systems.

REFERENCES

[1] J. D. Downie, J. E. Hurley, D. V. Kuksenkov, C. M. Lynn, A. E. Korolev, and V. N. Nazarov, "Transmission of 112 Gb/s PM-QPSK signals over up to 635 km of multimode optical fiber," *Opt. Exp.*, vol. 19, no. 26, pp. B363–B369, 2011.

[2] E. Ip, M.-J. Li, K. Bennett, Y.-K. Huang, A. Tanaka, A. Korolev, K. Koreshkov, W. Wood, E. Mateo, J. Hu, and Y. Yano, "146λ × 6 × 19-gbaud wavelength-and mode-division multiplexed transmission over 10 × 50-km spans of few-mode fiber with a gain-equalized few-mode EDFA," *J. Lightw. Technol.*, vol. 32, no. 4, pp. 790–797, Feb. 2014.

[3] J. van Weerdenburg, R. Ryf, J. C. Alvarado-Zacarias, R. A. Alvarez-Aguirre, N. K. Fontaine, H. Chen, R. Amezcua-Correa, Y. Sun, L. Grüner-Nielsen, R. V. Jensen, R. Lingle, T. Koonen, and C. Okonkwo, "138-Tb/s mode- and wavelength-multiplexed transmission over six-mode graded-index fiber," *J. Lightw. Technol.*, vol. 36, no. 6, pp. 1369–1374, Mar. 15, 2018.

[4] H. Zhong, S. Zou, D. Huang, and Y. Guo, "Continuous-variable quantum key distribution coexisting with classical signals on few-mode fiber," *Opt. Exp.*, vol. 29, no. 10, pp. 14486–14504, 2021.

[5] Y. Xie, L. Pei, J. Zheng, Q. Zhao, T. Ning, and J. Li, "Design of steering wheel-type ring depressed-core 10-mode fiber with fully improved mode spacing," *Opt. Exp.*, vol. 29, no. 10, pp. 15067–15077, 2021.

[6] S. Jiang, L. Ma, Z. Zhang, X. Xu, S. Wang, J. Du, C. Yang, W. Tong, and Z. He, "Design and characterization of ring-assisted few-mode fibers for weakly coupled mode-division multiplexing transmission," *J. Lightw. Technol.*, vol. 36, no. 23, pp. 5547–5555, Dec. 1, 2018.

[7] L. Gruner-Nielsen, Y. Sun, J. W. Nicholson, D. Jakobsen, K. G. Jespersen, R. Lingle, and B. Palsdottir, "Few mode transmission fiber with low DGD, low mode coupling, and low loss," *J. Lightw. Technol.*, vol. 30, no. 23, pp. 3693–3698, Dec. 2012.

[8] T. Mori, T. Sakamoto, M. Wada, T. Yamamoto, and F. Yamamoto, "Six-LP-mode transmission fiber with DMD of less than 70 ps/km over C+L band," in *Proc. Opt. Fiber Commun. Conf.* San Francisco, CA, USA: Optical Society of America, 2014, pp. 1–3, Paper M3F.3.

[9] P. Sillard, M. Bigot-Astruc, and D. Molin, "Few-mode fibers for mode-division multiplexed systems," *J. Lightw. Technol.*, vol. 32, no. 16, pp. 2824–2829, Aug. 15, 2014.

[10] P. Sillard, D. Molin, M. Bigot-Astruc, K. De Jongh, F. Achten, A. M. Velázquez-Benítez, R. Amezcua-Correa, and C. M. Okonkwo, "Low-differential-mode-group-delay 9-LP-mode fiber," *J. Lightw. Technol.*, vol. 34, no. 2, pp. 425–430, Jan. 15, 2016.

[11] D. W. Peckham, Y. Sun, A. McCurdy, R. Lingle Jr., I. Kaminow, T. Li, and A. E. Willner, *Few-Mode Fiber Technology for Spatial Multiplexing.* Amsterdam, The Netherlands: Elsevier, 2013, pp. 283–320.

[12] P. Sillard, D. Molin, M. Bigot-Astruc, A. Amezcua-Correa, K. de Jongh, and F. Achten, "50 μm multimode fibers for mode division multiplexing," *J. Lightw. Technol.*, vol. 34, no. 8, pp. 1672–1677, Apr. 15, 2016.

[13] P. Sillard, D. Molin, M. Bigot-Astruc, K. de Jongh, F. Achten, J. E. Antonio-López, and R. Amezcua-Correa, "Micro-bend-resistant low-differential-mode-group-delay few-mode fibers," *J. Lightw. Technol.*, vol. 35, no. 4, pp. 734–740, Feb. 15, 2017.

[14] H. Zhang, J. Zhao, Z. Yang, G. Peng, and Z. Di, "Low-DMGD, large-effective-area and low-bending-loss 12-LP-mode fiber for mode-division-multiplexing," *IEEE Photon. J.*, vol. 11, no. 4, pp. 1–8, Aug. 2019.

[15] F. M. Ferreira, D. Fonseca, and H. J. A. D. Silva, "Design of few-mode fibers with M-modes and low differential mode delay," *J. Lightw. Technol.*, vol. 32, no. 3, pp. 353–360, Feb. 2014.

[16] L. de Montmorillon, F. Gooijer, N. Montaigne, S. Geerings, D. Boivin, L. Provost, and P. Sillard, "All-solid G.652.D fiber with ultra low bend losses down to 5 mm bend radius," in *Proc. Opt. Fiber Commun. Conf. Nat. Fiber Opt. Eng. Conf., OSA Tech. Dig. (CD)*. Washington, DC, USA: Optica Publishing Group, 2009, pp. 1–3, Paper OTuL3.

[17] D. Molin, M. Bigot-Astruc, K. de Jongh, and P. Sillard, "Trench-assisted bend-resistant OM4 multi-mode fibers," in *Proc. 36th Eur. Conf. Exhib. Opt. Commun.*, Sep. 2010, pp. 1–3.

[18] T. Mori, T. Sakamoto, M. Wada, T. Yamamoto, and K. Nakajima, "Few-mode fiber technology for mode division multiplexing," *Opt. Fiber Technol.*, vol. 35, pp. 37–45, Feb. 2017.

[19] K.-I. Kitayama and N.-P. Diamantopoulos, "Few-mode optical fibers: Original motivation and recent progress," *IEEE Commun. Mag.*, vol. 55, no. 8, pp. 163–169, Aug. 2017.

[20] P. Shao, Z. Li, L. Ma, C. Wang, S. Li, J. Li, and T. Cheng, "Weakly coupled graded index heterogeneous nineteen-core few-mode fiber," *Opt. Exp.*, vol. 31, no. 6, pp. 10473–10488, 2023.

[21] J. Van Weerdenburg, A. Velàzquez-Benitez, R. van Uden, P. Sillard, D. Molin, A. Amezcua-Correa, E. Antonio-Lopez, M. Kuschnerov, F. Huijskens, H. de Waardt, T. Koonen, R. Amezcua-Correa, and C. Okonkwo, "10 spatial mode transmission using low differential mode delay 6-LP fiber using all-fiber photonic lanterns," *Opt. Exp.*, vol. 23, no. 19, pp. 24759–24769, 2015.

[22] J. W. Fleming, "Dispersion in GeO$_2$–SiO$_2$ glasses," *Appl. Opt.*, vol. 23, no. 24, pp. 4486–4493, 1984.

[23] V. Brückner, "To the use of Sellmeier formula," Senior Experten Service (SES) Bonn, HfT Leipzig, Bonn, Germany, Tech. Rep., 2011, pp. 242–250, vol. 42.

[24] J. Han, G. Gao, Y. Zhao, and S. Hou, "Bend performance analysis of few-mode fibers with high modal multiplicity factors," *J. Lightw. Technol.*, vol. 35, no. 13, pp. 2526–2534, Jul. 1, 2017.

[25] H. Zhang, G. Wang, J. Zhang, F. Wang, X. Yan, X. Zhang, and T. Cheng, "Design and optimization of a single-mode multi-core photonic crystal fiber with the nanorod assisted structure to suppress the crosstalk," *IEEE Photon. J.*, vol. 13, no. 4, pp. 1–6, Aug. 2021.

[26] X. Xie, J. Tu, X. Zhou, K. Long, and K. Saitoh, "Design and optimization of 32-core rod/trench assisted square-lattice structured single-mode multi-core fiber," *Opt. Exp.*, vol. 25, no. 5, pp. 5119–5132, 2017.

[27] T. Sakamoto, S. Aozasa, T. Mori, M. Wada, T. Yamamoto, S. Nozoe, Y. Sagae, K. Tsujikawa, and K. Nakajima, "Randomly-coupled single-mode 12-core fiber with highest core density," in *Proc. Opt. Fiber Commun. Conf. Exhib. (OFC)*, Los Angeles, CA, USA, Mar. 2017, pp. 1–3.

[28] K. Igarashi, D. Souma, Y. Wakayama, K. Takeshima, Y. Kawaguchi, T. Tsuritani, I. Morita, and M. Suzuki, "114 space-division-multiplexed transmission over 9.8-km weakly-coupled-6-mode uncoupled-19-core fibers," in *Proc. Opt. Fiber Commun. Conf. Post Deadline Papers*. Los Angeles, CA, USA: Optical Society of America, 2015, pp. 1–3, Paper Th5C.4.

[29] P. Shao, S. Li, X. Meng, Y. Guo, L. Wang, Z. Li, L. Ma, J. Li, T. Cheng, W. Xu, Y. Qin, and H. Zhou, "Low crosstalk and large effective mode field area heterogeneous 13-core 6-mode fiber with double high refractive index rings," *Opt. Commun.*, vol. 530, Mar. 2023, Art. no. 129136.

[30] Z. Li, L. Wang, Y. Wang, S. Li, X. Meng, Y. Guo, G. Wang, H. Zhang, T. Cheng, W. Xu, Y. Qin, and H. Zhou, "Manufacturable low-crosstalk high-RCMF 13-core 5-LP mode fiber with graded-index core and stairway-index trench," *Opt. Exp.*, vol. 29, no. 17, pp. 26418–26432, 2021.

YUHENG XIE received the Ph.D. degree in communication and information systems from Beijing Jiaotong University, Beijing, China, in 2022. He is currently a Researcher with the Institute of Basic Operations Technology, China Telecom Research Institute, Beijing. His research interests include quantum key distribution, quantum secure communication, special optical fiber, and optical fiber transmission systems.

JIANJUN TANG received the Ph.D. degree from the Beijing University of Posts and Telecommunications, Beijing, China. He is currently a Senior Engineer and the Team Director with the Institute of Basic Operations Technology, China Telecom Research Institute, Beijing. His research interests include quantum key distribution, quantum secure communication, and large-capacity optical transmission systems.

QI ZHAO received the Ph.D. degree in communication and information systems from Beijing Jiaotong University, Beijing, China, in 2022. She is currently a Researcher with the Institute of Basic Operations Technology, China Telecom Research Institute, Beijing. Her research interests include quantum key distribution, optical fiber amplifier, and optical fiber laser.

LIPENG FENG received the Ph.D. degree from the Beijing University of Posts and Telecommunications, Beijing, China, in 2021. She is currently a Researcher with the Institute of Network Technology, China Telecom Research Institute, Beijing. Her research interests include few-mode fiber and optical fiber communication systems.

TIANQI DOU received the Ph.D. degree from the Beijing University of Posts and Telecommunications, Beijing, China, in 2021. She is currently a Researcher with the Institute of Basic Operations Technology, China Telecom Research Institute, Beijing. Her recent research interests include quantum key distribution and quantum secure communication.

• • •